ISSN 0869-5911, Petrology, 2006, Vol. 14, No. 1, pp. 21–38. © Pleiades Publishing, Inc., 2006.
Original Russian Text © S.D. Velikoslavinsky, A.B. Kotov, E.B. Sal'nikova, V.P. Kovach, V.A. Glebovitsky, N.Yu. Zagornaya, S.Z. Yakovleva, E.V. Tolmacheva, I.V. Anisimova, A.M. Fedoseenko, 2006, published in Petrologiya, 2006, Vol. 14, No. 1, pp. 25–43.

Protoliths of the Metamorphic Rocks of the Fedorov Complex, Aldan Shield: Character, Age, and Geodynamic Environments of Origin

S. D. Velikoslavinsky*, A. B. Kotov*, E. B. Sal'nikova*, V. P. Kovach*, V. A. Glebovitsky*, N. Yu. Zagornaya*, S. Z. Yakovleva*, E. V. Tolmacheva, I. V. Anisimova*, and A. M. Fedoseenko***

**Institute of Precambrian Geology and Geochronology (IGGD), Russian Academy of Sciences, nab. Makarova 2, St. Petersburg, 199034 Russia*
e-mal: sdtj@sv1403.spb.edu
***Karpinskii All-Russia Research Institute of Geology (VSEGEI), Srednii pr. 74, St. Petersburg, 199026 Russia*

Received September 24, 2004

Abstract—Geochemical data indicate that the protoliths of the overwhelming majority of the metamorphic rocks composing the Fedorov Complex in the Aldan granulite megacomplex were volcanic rocks of three groups, which occur in different proportions in the complex: (i) volumetrically predominant (no less than 90%) continuous differentiated island-arc basalt–andesite–dacite–rhyolite series, (ii) within-plate basalts, whose composition was similar to that of low-Ti traps, and (iii) basalts of composition similar to that of continental-rift basalts. The U–Pb zircon crystallization age of the metamorphosed basaltic andesites of the Fedorov Complex was estimated at 2006 ± 3 Ma, which testifies, when considered together with preexisting geochronological data, that the complex was produced during a time span of no longer than 25 m.y. A model is proposed according to which the complex was produced within the geodynamic system of the active continental margin of the Olekma–Aldan continental microplate and the Fedorov island arc.

DOI: 10.1134/S0869591106010036

INTRODUCTION

The past decade witnessed the amassing of geochronologic and isotopic geochemical data (Kotov *et al.*, 1993, 1995a; 1995b, 1999, 2004; Kovach *et al.*, 1996a, 1996b, 1999, 2000; Kotov, 2003; Larin *et al.*, 2000, 2002; Salnikova *et al.*, 1993, 1996, 1997; Frost *et al.*, 1998; Nutman *et al.*, 1992; Neymark *et al.*, 1993), which resulted in the revision of several aspects of the traditional concepts for the Early Precambrian evolution of the Aldan Shield. At the same time, some aspects of the geology and petrology of the regional Precambrian complexes, including the problem of the age and genesis of metamorphic rock sequences of the Aldan geoblock (Aldan granulite–gneiss terrane), remain uncertain as of yet. In this context, this paper discusses currently available geological, geochronological, geochemical, and isotopic geochemical data that make it possible to date the metamorphic rocks of the Fedorov Complex of the Aldan granulite–gneiss terrane (to which several mineral deposits and occurrences of the Aldan phlogopite province are restricted) and provide insight into the geodynamic environment in which these rocks were formed. The complex is one of the few high-grade supracrustal metamorphic complexes of the Aldan Shield for which data were obtained (Velikoslavinsky *et al.*, 1995; Velikoslavinsky, 1998) indicating that the rocks had been formed in a subduction environment. Because of this, the problems listed above are crucial for geodynamic models of the origin and evolution not only of the Aldan geoblock but also of the whole Aldan Shield.

GEOLOGY

The Fedorov Complex was first distinguished by S.P. Konoplev in 1948 (*Early Precambrian...*, 1986) and thereafter was included (practically without any changes in the scope) as a formation or group in all stratigraphic schemes proposed for the Aldan granulite–gneiss megacomplex. Over more than 50 years of studying the Aldan Shield, the concepts of the stratigraphy of the Fedorov Complex and its position in the overall stratigraphic scheme of the Aldan megacomplex were significantly changed. Originally, following the proposal of Yu.K. Dzevanovskii (1958), it was regarded as the uppermost formation of the oldest Iengra Group, which conformably overlies the Nimnyr Formation of enderbite and charnockite granite-gneisses (Korzhinskii, 1936; Verevkin *et al.*, 1966). Later, the Fedorov Complex was recognized as a formation in the bottom part of the Timpton Group (*Geological Map...*, 1988; and others), included in the Timpton Subgroup (Salop

and Travin, 1974), or was considered to be a large individual stratigraphic unit—the Fedorov Group (Rudnik, 1975; Velikoslavinsky, 1978; and others). In the stratigraphic scheme of the stratified high-grade metamorphic rocks of the central Aldan Shield proposed by V.L. Duk *et al.* (*Early Precambrian…*, 1986; *Precambrian Geology…*, 1988), which was based on the study of natural mineral assemblages of the metamorphic rocks and the petrochemical reconstructions of their protoliths, the Fedorov, Seimskii, Kholbolokh, Chuga, Kyurikan, and Idzhek stratigraphic units were ascribed to the upper tectonic–stratigraphic complex, and the Kurulta, Zverev, Kurumkan, and Amedichi units were regarded as composing the lower complex.

According to Duk (1994), the rocks of the Fedorov Complex compose the so-called Fedorov Allochthon. Fragments of this allochthon preserved at the modern erosion level account for approximately 30% of the Aldan geoblock of the Aldan Shield by area and are restricted to its western part (Fig. 1). The field of widespread metamorphic rocks of the Fedorov Complex is bounded by the Timpton Thrust in the east and extends practically to the Aldan–Kilier fault zone in the west (Fig. 1). The latter is considered to be the eastern boundary of the junction zone of the Chara–Olekma geoblock (Olekma granite–greenstone terrane) and the Aldan geoblock (Sal'nikova *et al.*, 1996; Kotov, 2003).

The Fedorov Complex consists of predominantly hypersthene (±biotite, ±amphibole, ±diopside) plagioclase gneisses and gneisses with subordinate amounts (close to 20%) of hornblende–plagioclase, diopside–hornblende–plagioclase, and hypersthene–diopside–hornblende–plagioclase mafic schists with occasional layers and lenses of diopside and phlogopite–diopside, and diopside–plagioclase rocks, calciphyres, marbles, and rare intercalations of garnet–biotite plagioclase gneisses. It cannot be ruled out that the marbles and calciphyres of the Fedorov Complex, as well as the phlogopite–diopside and diopside–plagioclase rocks, were produced by the processes of Mg–Fe–Ca metasomatism, which were widespread in the Fedorov Complex and produced numerous mineral deposits and occurrences of phlogopite and iron. The thickness of the Fedorov Complex is uncertain and reportedly ranges in various publications from 960–1200 m (Petrova *et al.*, 1975) to 2700–4800 m (Verevkin *et al.*, 1966).

The rocks of the Fedorov Complex underwent structural–metamorphic alterations. They were originally metamorphosed to the high-grade granulite facies and then were overprinted by metamorphism under conditions transitional from the granulite to amphibolite facies (*Early Precambrian…*, 1986).

ANALYTICAL TECHNIQUES

The major-element analyses of rocks from the Fedorov Complex reported in this paper were conducted by XRF at the Karpinskii All-Russia Research Institute of Geology. The rocks were analyzed for REE by instrumental neutron activation at the St. Petersburg State University accurate to 5–15%. Rb was determined by flame photometry at the Karpinskii All-Russia Research Institute of Geology, and other trace elements were determined by spectral analysis (with an external standard) at the same institute. Some representative rock samples from the Fedorov Complex were analyzed for trace elements by ICP-MS accurate to 5–10% (at IAnP of the St. Petersburg Research Center, Russian Academy of Sciences).

Accessory minerals were separated by the conventional techniques with the use of heavy liquids. The decomposition of the samples and the chemical extraction of Pb and U were conducted by a modified method (Krogh, 1973). The blanks did not exceed 50 pg for Pb and 5 pg for U. The Pb and U isotopic composition was determined on a Finnigan MAT-261 mass spectrometer in static mode. The U/Pb ratio was measured accurate to 0.5%. The preliminary acid ($HF + HNO_3$) treatment was conducted at different exposures at a temperature of 220°C (Mattinson, 1994). The experimental data were processed by the PbDAT (Ludwig, 1991) and ISOPLOT (Ludwig, 1999) computer programs. The age values were calculated using the conventionally adapted U decay constants (Steiger and Jager, 1976). The corrections for common Pb were introduced in compliance with the model values (Stacey and Kramers, 1975). All errors are reported for 2σ levels.

Sm and Nd were extracted by the method described in (Kotov *et al.*, 1995). The measured $^{143}Nd/^{144}Nd$ ratio was normalized to $^{146}Nd/^{144}Nd = 0.7219$ and brought to the ratio $^{146}Nd/^{144}Nd = 0.511860$ in the La Jolla Nd standard. The accuracy of the measured Sm and Nd concentrations is 0.5%, and those of the $^{147}Sm/^{144}Nd$ and $^{143}Nd/^{144}Nd$ isotopic ratios are 0.5 and 0.005%, respectively (2σ). The weighted mean values of the $^{143}Nd/^{144}Nd$ ratio in the La Jolla Nd standard is 0.511873 ± 11 (eight measurements). The blanks during the experiment were 0.03–0.2 ng for Sm and 0.1–0.5 ng for Nd. The values of $\varepsilon_{Nd}(0)$ and model ages $T_{Nd}(DM)$ were calculated using the modern values for CHUR (Jacobsen and Wasserburg, 1984) and DM (Goldstein and Jacobsen, 1988). The two-stage model ages $T_{Nd}(DM\text{-}2st)$ (Liew and Hofmann, 1988) were calculated with assumed $^{147}Sm/^{144}Nd = 0.12$ (Taylor and McLennan, 1985).

PROTOLITHS OF THE METAMORPHIC ROCKS OF THE FEDOROV COMPLEX

The composition of rocks composing the Fedorov Complex was thoroughly studied (Duk *et al.*, 1975; Travin, 1974; Petrova *et al.*, 1975; Velikoslavinsky, 1978; Velikoslavinsky and Rudnik, 1983; Petrova and Levitskii, 1986; *Early Precambrian…*, 1986; Velikoslavinsky, 1998; and others), largely because the complex hosts phlogopite and iron deposits. Because of this we quote (Tables 1, 2) only representative analytical

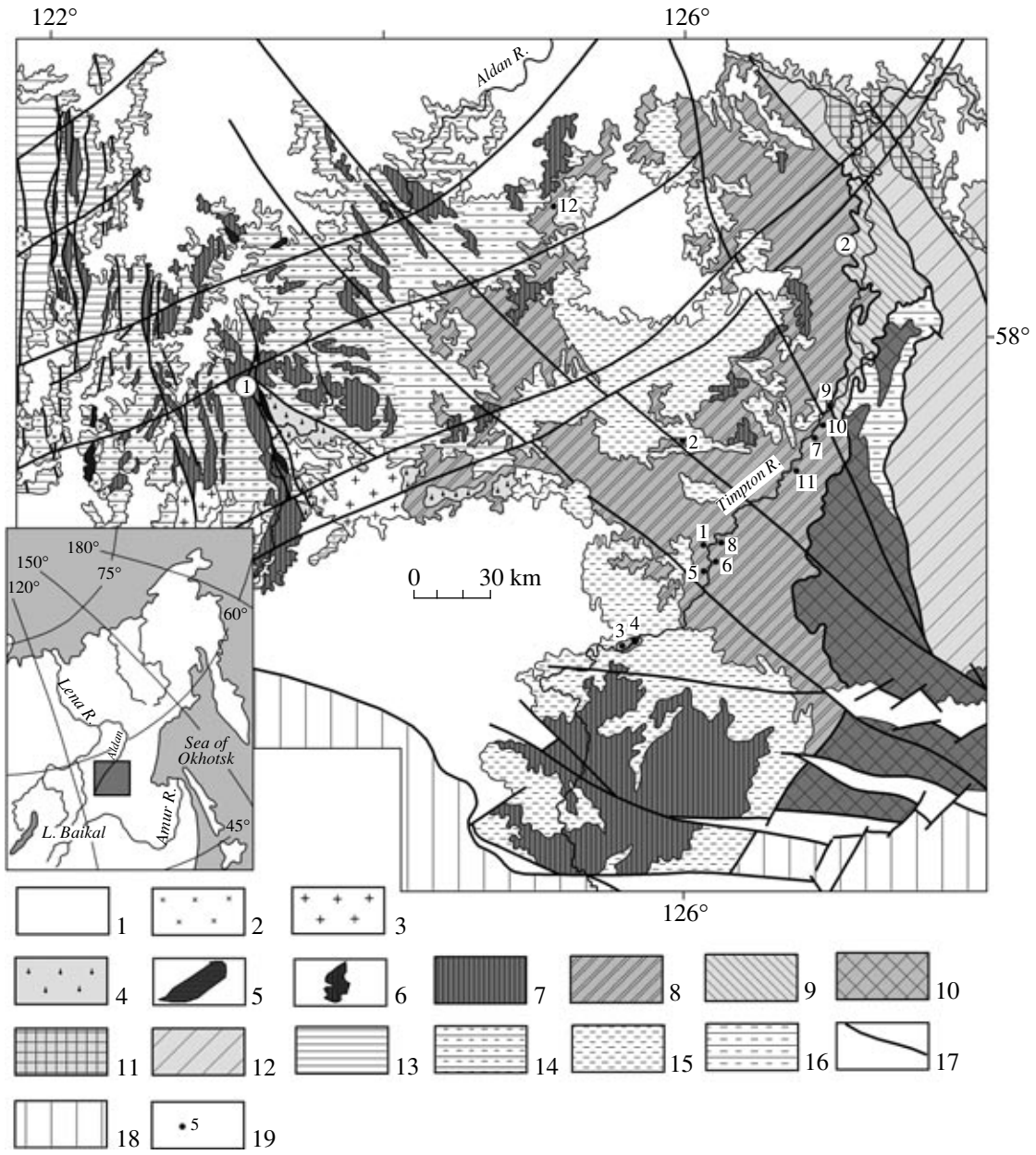

Fig. 1. Schematic geological map of the central part of the Aldan Shield.

(1) Quaternary, Mesozoic, Paleozoic, and Upper Proterozoic platform-cover deposits; (2) undifferentiated Early Proterozoic granites (Amut and other complexes); (3) granites, Dzhaltunda Complex; (4) magmatic rocks of the Ungra Complex; (5) low-grade metamorphic volcanic–sedimentary deposits of the Balaganakh greenstone belt; (6) metasedimentary and metavolcanic rocks of the Subgan Complex; (7–12) high-grade metamorphic volcanic–sedimentary deposits of the Aldan granulite–gneiss megacomplex: (7) undifferentiated Kurumkan, Amedichi, and Chuga complexes (predominantly garnet–cordierite–biotite, garnet–sillimanite–cordierite–biotite, sillimanite–biotite, cordierite–sillimanite–biotite gneisses, quartzites, two-pyroxene–hornblende and diopside–hornblende mafic schists), (8) Fedorov Complex (hypersthene–biotite, hypersthene–biotite–hornblende, biotite–hornblende, two-pyroxene–hornblende, and diopside–hornblende plagioclase gneisses, two-pyroxene–hornblende, diopside–hornblende, and hornblende mafic schists with occasional calciphyre intercalations), (9) Idzhek Complex (hypersthene, hypersthene–diopside, and hypersthene–diopside–hornblende plagioclase gneisses with intercalations and lenses of hypersthene–diopside and hypersthene–diopside–hornblende mafic schists, diopside–scapolite and diopside-plagioclase schists with thin intercalations of garnet-biotite and garnet–hypersthene–biotite gneisses), (10) Seim Complex (garnet–biotite gneisses and plagioclase gneisses, aluminous sillimanite–cordierite–garnet gneisses, two-pyroxene and diopside–hornblende plagioclase gneisses, and quartzites with rare interbeds of calc–silicate rocks); (11) Kyurikan Complex (cyclically intercalating garnet–biotite, hypersthene–biotite, biotite, hypersthene–diopside, and hypersthene–diopside–hornblende plagioclase gneisses, marbles, calciphyres, diopside and diopside–hornblende mafic schists), (12) Kholbolokh association (garnet–biotite plagioclase gneisses with rare interbeds of calc–silicate rocks; hypersthene, diopside, and two-pyroxene plagioclase gneisses with beds of mafic schists, marbles, and calciphyres); (13) granite-gneisses of the Olekma Complex; (14) granite-gneisses of the Timpton Complex; (15) granite-gneisses of the Aldan Complex; (16) undifferentiated granite-gneisses of the Aldan and Timpton Complex; (17) faults; (18) junction zone of the Aldan Shield and Dzhugdzhur–Stanovoi foldbelt; (19) sites of sampling for Sm–Nd isotopic–geochemical and U–Pb geochronological studies (numbers correspond to those in Table 4). Circled numerals: (1) Aldan–Kilier fault zone; (2) Timpton overthrust.

The inset shows the location of the study area.

Table 1. Chemical composition of representative samples of metamorphic rocks from the Fedorov Complex

Component	Mafic schists									Hypersthene gneisses		
	type I			type II					type III			
	V-133	1862	V-137	V-132	1822	1826	V-20b	P-2369/1	V-9a	1857	1860a	P-2388
SiO_2	48.03	49.08	49.57	45.34	47.08	49.37	49.69	50.88	44.48	53.64	54.50	54.79
TiO_2	1.25	1.10	1.05	1.00	1.76	1.06	0.90	0.69	1.55	0.935	1.00	1.21
Al_2O_3	17.82	16.24	18.95	13.38	14.18	13.16	11.74	12.65	18.76	17.75	16.35	17.81
Fe_2O_3	4.55	6.34	4.95	4.01	9.23	7.27	2.27	3.67	9.76	7.71	5.64	3.93
FeO	6.96	5.30	5.11	7.62	7.38	7.17	6.75	7.29	8.66	–	3.99	4.34
FeO_t	11.06	11.01	9.57	11.23	15.69	13.17	8.79	10.59	17.44	6.94	9.07	7.88
MnO	0.14	0.21	0.08	0.19	0.26	0.31	0.29	0.26	0.14	0.13	0.12	0.16
MgO	5.95	6.02	4.00	10.76	5.16	6.77	10.49	9.66	3.94	4.75	4.33	3.64
CaO	9.86	8.41	8.87	11.68	9.68	8.94	11.16	10.17	6.9	7.47	7.29	6.97
Na_2O	4.00	3.98	4.84	2.34	3.42	3.34	2.84	3.06	4.39	4.92	3.20	4.87
K_2O	1.49	1.43	1.40	2.29	0.89	1.09	1.69	1.05	1.5	1.75	1.89	0.84
P_2O_5	0.35	0.34	0.36	0.48	0.10	0.05	0.25	0.19	0.33	0.33	0.47	0.26
LOI	1.05	0.98	0.74	1.32	0.81	1.17	1.62	1.21	0.48	0.45	0.68	0.53
Total	101.45	99.44	99.92	100.41	99.95	99.95	99.69	100.77	100.92	99.84	99.46	99.35
Ba	–	–	–	700	–	–	370	–	260	494	–	370
Sr	–	–	–	560	–	–	420	–	250	–	–	370
V	–	–	–	270	–	–	230	205	360	112	–	100
Zr	–	–	–	190	–	–	320	112	230	–	–	300
Pb	–	–	–	9	–	–	18	–	14	–	–	10
Cr	–	–	–	140	–	–	180	120	250	98	–	52
Ni	–	–	–	280	–	–	400	70	200	–	–	25
Ga	–	–	–	15	–	–	20	–	32	–	–	28
Y	–	–	–	30	–	–	36	–	47	–	–	21
Zn	–	–	–	130	–	–	160	–	160	–	–	3
Sc	–	–	–	40	–	–	43	–	50	–	–	10
Co	–	–	–	52	–	–	40	28	58	–	–	20
Yb	–	–	–	–	–	–	–	–	–	–	–	2.4
Nb	–	–	–	–	–	–	–	–	–	–	–	12
Rb	–	–	–	116	–	–	81	14	–	–	–	6.4
La	–	–	–	46	–	–	46.0	50.0	–	–	–	–
Ce	–	–	–	71	–	–	62.1	113.0	–	–	–	–
Nd	–	–	–	–	–	–	36.7	51.5	–	–	–	–
Sm	–	–	–	6.34	–	–	6.37	9.51	–	–	–	–
Eu	–	–	–	1.27	–	–	1.75	2.05	–	–	–	–
Tb	–	–	–	0.59	–	–	0.69	0.94	–	–	–	–
Yb	–	–	–	1.36	–	–	1.87	2.71	–	–	–	–

Table 1. (Contd.)

Component	Hypersthene gneisses										
	1387a	1890	P-2368	1866	P-2056	1908b	P-2058	V-1216	1907a	1880g	B-2880/1
SiO_2	55.63	60.76	62.03	65.11	65.27	66.38	68.24	68.70	71.98	75.10	68.02
TiO_2	0.61	0.48	0.53	0.49	0.36	0.39	0.52	0.33	0.27	0.21	0.46
Al_2O_3	17.02	16.24	15.97	16.83	16.53	17.67	14.36	15.58	15.05	13.34	14.79
Fe_2O_3	4.09	3.56	3.39	4.15	2.62	2.06	1.07	1.66	1.60	2.00	1.02
FeO	5.11	4.67	3.81	2.57	0.78	2.42	3.09	0.79	1.42	0.80	4.02
FeO_t	8.79	7.87	6.86	6.31	3.14	4.27	5.02	2.29	2.86	2.60	4.94
MnO	0.12	0.15	0.14	0.15	0.05	0.06	0.06	0.02	0.07	0.05	0.09
MgO	2.84	2.97	3.72	1.77	1.75	1.70	3.13	0.61	0.71	0.91	1.40
CaO	7.31	5.98	4.65	4.46	3.00	4.24	3.86	2.35	2.25	3.04	4.17
Na_2O	5.33	3.20	4.2	4.06	5.90	4.06	3.77	4.86	3.54	3.22	3.43
K_2O	1.12	1.00	1.48	0.82	2.88	1.05	1.57	4.14	2.53	1.55	2.02
P_2O_5	0.22	0.13	0.13	0.17	0.16	0.15	0.27	0.09	0.05	–	–
LOI	0.71	0.71	0.58	0.70	0.65	0.43	1.06	0.57	0.38	0.69	0.65
Total	100.11	99.85	100.63	101.28	99.95	100.61	101.00	99.70	100.85	100.91	100.07
Ba	–	–	580	–	–	–	–	1300	–	–	–
Sr	–	–	250	–	–	–	–	1900	–	–	–
V	–	–	130	–	–	–	–	62	–	–	–
Zr	–	–	110	–	–	–	–	220	–	–	–
Pb	–	–	8.5	–	–	–	–	8	–	–	–
Cr	–	–	42	–	–	–	–	26	–	–	–
Ni	–	–	10	–	–	–	–	13	–	–	–
Ga	–	–	18	–	–	–	–	25	–	–	–
Y	–	–	28	–	–	–	–	8	–	–	–
Zn	–	–	100	–	–	–	–	–	–	–	–
Sc	–	–	19	–	–	–	–	3	–	–	–
Co	–	–	17	–	–	–	–	10	–	–	–
Yb	–	–	2.2	–	–	–	–	0.7	–	–	–
Nb	–	–	10	–	–	–	–	8	–	–	–
Rb	–	–	63.7	–	–	–	–	77.7	–	–	–
La	–	–	–	–	–	–	–	–	–	–	–
Ce	35.0	–	39.6	–	62.8	–	36.5	–	–	–	–
Nd	20.4	–	20.7	–	32.6	–	18.0	–	–	–	–
Sm	4.21	–	3.98	–	5.8	–	3.21	–	–	–	–
Eu	1.43	–	1.25	–	1.74	–	0.96	–	–	–	–
Tb	0.49	–	0.44	–	0.69	–	0.32	–	–	–	–
Yb	1.7	–	1.82	–	2.64	–	1.02	–	–	–	–

Note: Samples: V-133—*Hbl–Pl* mafic schist with *Mag,* Burdykhlai Creek; 1862—*Opx–Cpx–Hbl–Pl* mafic schist, left bank of the Timpton River, 16.8 km downstream of the Oyumrak River; V-137—*Hbl–Pl* mafic schist with *Mag* and *Bt*, Snezhnyi Mine; V-132—*Cpx–Hbl–Pl* mafic schist with *Mag* and *Bt*, Burdykhlai Creek; 1822—*Cpx–Hbl–Pl* mafic schist with *Mag*, left bank of the Timpton River, 10.7 km downstream of the Burnyi Creek; 1826—*Hbl–Cpx–Pl* mafic schist with *Mag*, left bank of the Timpton River, 4.5 km downstream of the Amnunakta River; V-20b—*Hbl–Pl* mafic schist, Timpton River, 21 km downstream of the Bezymyannyi Creek; P-2369/1—*Opx–Cpx–Hbl–Pl* mafic schist, Katalakh Creek; V-9a—*Opx–Cpx–Hbl–Pl* mafic schist with *Mag*, Timpton River, 7.5 km downstream of the Bezymyannyi Creek; 1857—*Bt–Hbl–Opx–Pl–Qtz* melanocratic plagioclase gneiss, left bank of the Timpton River, 7.2 km downstream of the Oyumrak River; 1860a—*Opx–Cpx–Hbl* plagioclase gneiss, right bank of the Timpton River, 13.5 km downstream of the Oyumrak River; P-2388—*Bt–Opx* plagioclase gneiss, watershed area between the Katalakh and Pravaya Yllymakh rivers; 1387a—*Bt–Opx* plagioclase gneiss, Pravaya Yllymakh River; 1890—*Bt–Opx* plagioclase gneiss, right bank of the Timpton River, 3.5 km upstream of the Egete River; P-2368—*Bt–Opx* plagioclase gneiss, Katalakh Creek; 1866—*Bt–Opx* plagioclase gneiss, right bank of the Timpton River, 2 km downstream of the Khatyma River; P-2056—*Bt–Opx* plagioclase gneiss, near the village of Kanku; 1908b—*Bt–Opx* plagioclase gneiss, left bank of the Timpton River, 6 km upstream of the Tas-Khoonku River; P-2058—*Bt–Opx* plagioclase gneiss, near the village of Kanku; V-1216—*Bt–Opx* plagioclase gneiss, Bol'shoi Des River; 1907a—*Bt–Opx* plagioclase gneiss, right bank of the Timpton River, 5 km upstream of the Tas-Khoonku River; 1880g—*Bt–Opx–Cpx–Hbl* plagioclase gneiss, right bank of the Timpton River, 1.5 km upstream of the Nel'gou River; B-2880/1—*Opx–Hbl* plagioclase gneiss (metagraywacke), confluence of the Kuranakh and Koltykon rivers. Minerals: *Bt*—biotite, *Opx*—orthopyroxene, *Cpx*—clinopyroxene; *Pl*—plagioclase, *Mag*—magnetite, *Hbl*—hornblende, *Qtz*—quartz. Samples P-2369/1, P-2388, P-2368, and P-2058 are from T.A. Pavlova's collection; sample B-2880/1 is from V.I. Berezkin's collection. Trace elements were determined by quantitative spectral analysis (external standard) at Karpinskii All-Russia Research Institute of Geology, REE were analyzed by instrumental neutron activation at the St. Petersburg State University. Oxides are given in wt %, trace elements are in ppm, dashes mean not analyzed.

Table 2. Concentrations of trace elements (ppm) in representative samples of metamorphic rocks from the Fedorov Complex

Element	Mafic schists					Hypersthene gneisses	
	type I			type II			
	V-133	1862	V-137	1822	1826	1860a	1866
Sc	25	22	17.0	44	46	15.5	18.1
Ti	4884	5858	4598	8902	6027	5448	2798
V	171	217	154	302	316	167	109
Cr	53	55	13.2	32	159	23	16.3
Co	32	42	31	56	51	33	14.3
Ni	20.0	66	8.4	38	70	38	0.85
Cu	11.3	23	31	21	37	26	1.46
Rb	22	38	33	17.7	10.7	44	20
Sr	509	579	793	231	81	847	400
Ba	357	455	649	328	104	723	779
Y	16.6	18.4	18.1	31	28	14.7	19.5
Zr	49	141	70	87	55	131	149
Nb	6.7	13.7	8.0	9.4	6.3	17.1	11.6
Hf	1.52	3.7	1.58	2.2	1.77	3.4	3.3
Ta	0.58	1.34	0.44	0.88	0.53	1.66	0.80
Pb	15.8	5.2	8.2	14.8	4.0	6.1	7.1
Th	1.04	17.1	0.59	1.32	0.97	5.9	3.6
U	1.00	2.4	0.6	0.45	0.30	1.72	0.46
La	24.0	59	26.1	11.8	15.5	34	29
Ce	58	138	70	28.0	36	90	66
Pr	6.2	14.7	7.5	3.6	4.0	10.0	7.8
Nd	25.0	55	30.7	15.7	16.0	42	32.1
Sm	5.4	8.6	6.6	4.2	3.8	7.6	6.2
Eu	1.61	2.08	1.69	1.40	1.05	2.05	1.34
Gd	4.5	6.6	4.9	5.0	4.7	5.3	4.8
Tb	0.58	0.80	0.62	0.84	0.83	0.71	0.67
Dy	3.11	3.7	3.3	5.3	4.6	2.97	3.5
Ho	0.57	0.71	0.63	1.18	1.04	0.55	0.71
Er	1.70	1.93	1.78	3.5	3.3	1.50	2.17
Tm	0.26	0.24	0.23	0.50	0.49	0.21	0.29
Yb	1.52	1.45	1.41	3.35	3.08	1.24	1.89
Lu	0.22	0.25	0.21	0.49	0.45	0.19	0.28
$(La/Yb)_N$	10.6	27.6	12.5	2.4	3.4	18.4	10.3
$(La/Sm)_N$	2.8	4.3	2.5	1.8	2.5	2.8	2.9
$(Gd/Yb)_N$	2.4	3.7	2.8	1.2	1.2	3.4	2.0
Eu/Eu*	0.96	0.81	0.87	0.93	0.75	0.93	0.72
La/Nb	3.6	4.3	3.2	1.3	2.5	2.0	2.5

Note: See note to Table 1 for brief characteristics of the samples and their sampling sites. Elements were determined by ICP-MS.

data on major petrographic varieties composing this metamorphic complex: mafic schist and hypersthene gneisses, although the diagrams presented below are based on all available data (both original and compiled from the literature).

Mafic schists. The application of all known petrochemical techniques currently employed for identifying the protoliths of these rocks in various Precambrian stratigraphic units of the Aldan Shield, including the Fedorov Complex, leads to the conclusion that they chemically correspond to mafic magmatic rocks (Travin, 1974; Petrova *et al.*, 1975; Petrova and Levitskii, 1986; Velkoslavinsky, 1998; and others). The magmatic nature of the protoliths of both the mafic schists and the hypersthene gneisses of the Fedorov Complex is also confirmed by the results obtained by studying inclusions (Velikoslavinsky *et al.*, 1993; Tolmacheva and Velikoslavinsky, 1999), which indicate that the rock-forming minerals of these rocks contain premetamorphic high-temperature melt inclusions.

The chemical composition of the Fedorov mafic schists corresponds to those of subalkaline and alkaline basalts (Table 1, Figs. 2a, 2b) with normative nepheline. The petrochemical variability of the mafic schists generally corresponds to the Bowen differentiation trend (Fig. 2c), a fact that not only highlights the nature of the protoliths but also testifies to the nearly isochemical character of their metamorphism, because otherwise the preservation of the clear-cut compositional trend could hardly be possible.

The volcanic, but not intrusive, genesis of the protoliths of most of the mafic schists of the Aldan granulite–gneiss megacomplex, including the Fedorov mafic schists, also follows from the lithological control over their chemical composition (Velikoslavinsky, 1998): clear differences between the compositions of mafic schists in discrete stratigraphic units of the Aldan megacomplex, a fact that offers the possibility of the broad application of geochemical data to the solution of stratigraphic problems.

According to the chemistries of the mafic schists (metabasalts) of the Fedorov Complex, these rocks can be definitely subdivided into at least three groups, which have statistically significant differences in the contents of TiO_2, Al_2O_3, FeO_t, MnO, MgO, CaO, Cr, Ni, and Sr (Table 1, Figs. 2c, 3b). The complex is dominated by high-Al metabasalts (type I: 17.46 wt % Al_2O_3, 1.02 wt % TiO_2, 10.1 wt % FeO_t, and 5.55 wt % MgO). The complex contains subordinate amounts of more ferrous and magnesian but less aluminous metabasalts of type II (average concentrations: 14.14 wt % Al_2O_3, 1.20 wt % TiO_2, 12.08 wt % FeO_t, and 6.93 wt % MgO) and highly aluminous, highly titanic, and highly ferrous metabasalts of type III (average concentrations: 17.73 wt % Al_2O_3, 1.73 wt % TiO_2, and 13.0 wt % FeO_t).

In the Pearce diagram (Fig. 3a), most of the data points of the Fedorov metabasalts plot within the fields of arc calc–alkaline and low-K tholeiite basalts. Only about 5% of our samples plot within the MORB field, and 6% fall into the field of within-plate basalts. Inasmuch all metabasalts of the Fedorov Complex belong to alkaline and subalkaline varieties, and their K_2O concentrations vary from 0.6 to 3.6 wt %, there seem to be unreasonable to assign the samples that plot within the MORB field to analogues of MORB. Our earlier specialized research (Velikoslavinsky, 1997) has demonstrated that the Pearce discriminant diagram not always can accurately enough distinguish between arc and within-plate basalts. For example, the compositions of low-Ti flood basalts and, to a lesser degree, riftogenic basalts quite often plot in this diagram within the field of arc basalts. Because of this and also to reliably identify the tectonic environments in which the Fedorov metabasalts were produced, we used literature data on the compositions of basalts from island arc and continental-margin ($n = 773$), continental rifts ($n = 597$), and trap provinces ($n = 416$) to calculate two discriminant functions: D_x and D_y. The former differentiates arc and continental-margin basalts from continental-rift basalts (the weighted mean probability of an inaccurate classification is $R = 5.4\%$, the Mahanalobis distance is $D^2 = 2.98$), and the latter distinguishes arc and continental-margin basalts from flood basalts in trap provinces ($R = 9.1\%$, $D^2 = 2.51$). These values were used to construct a diagram (Velikoslavinsky and Glebovitsky, 2005) that can accurately enough discriminate between island-arc and within-plate basalts (Fig. 3b). In this diagram, and in Pearce's diagram, most (approximately to 80%) of the composition points of the Fedorov metabasalts that correspond to type-I basalts plot within the field of arc basalts. Approximately 15% of the data points (type-II metabasalts) correspond to within-plate basalts and show many similarities with flood basalts. Finally, 5% of the samples (type-III metabasalts) are compositionally analogous to continental-rift basalts.

The fractionation plots of trace elements and REE for representative samples of the type-I and type-II metabasalts are shown in Fig. 4. The type-I metabasalts are characterized by the strong fractionation of trace elements that are immobile during metamorphic processes, and their plots show negative anomalies at Nb, Ta (La/Nb = 3.2–4.3), Zr, Hf, and Ti (Fig. 4a). These rocks are characterized by moderately fractionated REE with enrichment in LREE and depletion in HREE [$(La/Yb)_N$ = 10.6–12.6], fractionated distribution of LREE and HREE [$(La/Sm)_N$ = 2.8–4.3, $(Gd/Yb)_N$ = 2.4–3.7], and weakly pronounced (if any) Eu anomalies (Eu/Eu* = 0.81–0.96) (Fig. 4b). This distribution of trace elements is typical of basalts in modern island arcs (Condie, 1977).

The type-II metabasalts have less fractionated trace-element patterns (La/Nb = 1.3–2.5) and less pronounced negative anomalies at Nb, Ta, Zr, Hf, and Ti (Fig. 4). The REE patterns (Fig. 5) are also fractionated less strongly [$(La/Yb)_N = 2.4–3.4$], the HREE patterns are gently sloping [$(La/Sm)_N = 1.8–2.5$, $(Gd/Yb)_N = 1.2$], and the negative Eu anomalies are poorly pronounced or

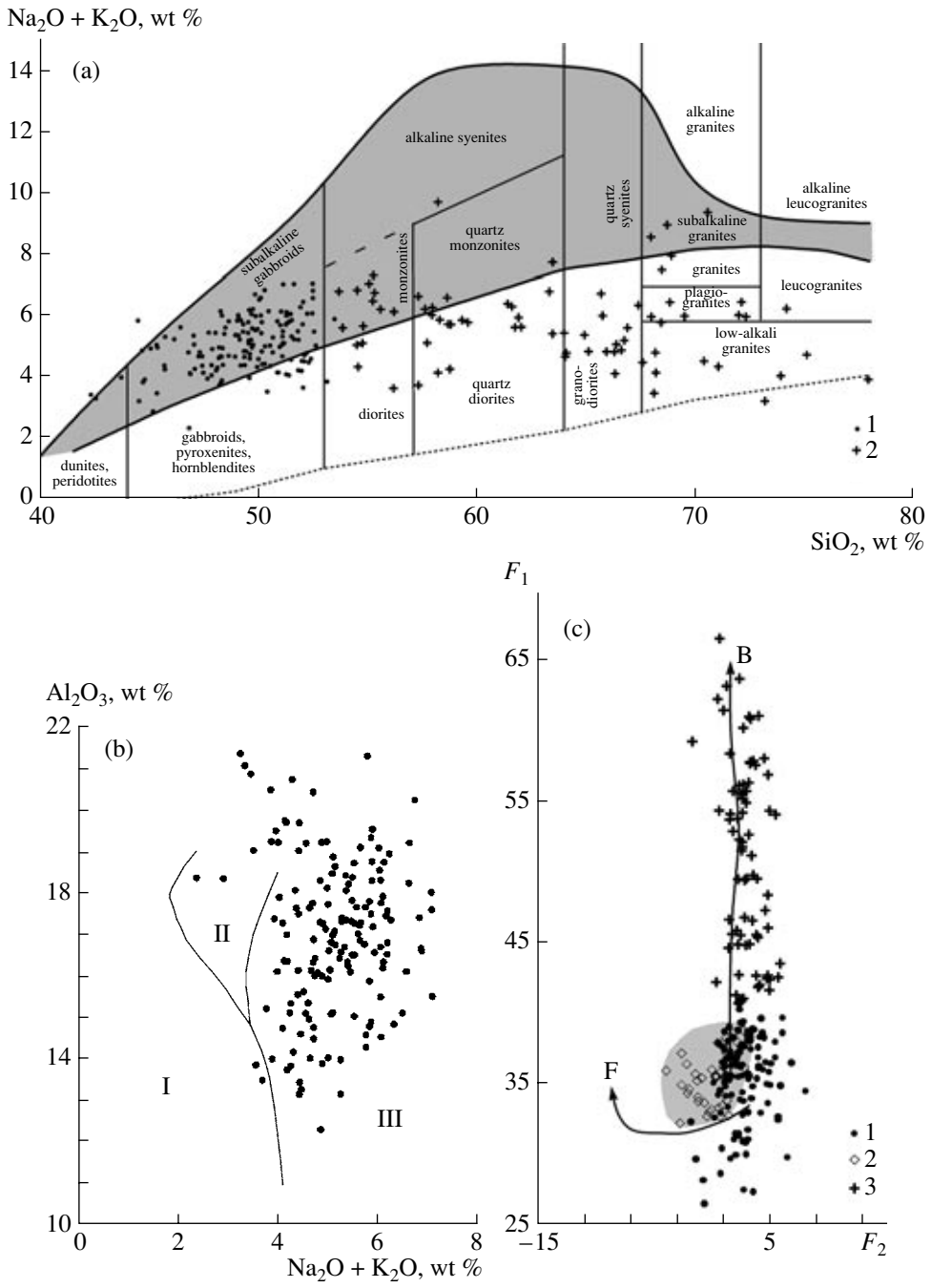

Fig. 2. Petrochemical diagrams illustrating the distinctive compositional features of metavolcanic rocks of the Fedorov Complex.
(a) ($Na_2O + K_2O$) vs. SiO_2 diagram (*Magmatic…*, 1983) for the metavolcanic rocks of the Fedorov Complex. (1) Mafic schists (metabasalts); (2) hypersthene gneisses (metavolcanic rocks of intermediate–acid composition).
(b) ($Na_2O + K_2O$) vs. Al_2O_3 diagram (Kuno, 1961) for the metabasalt of the Fedorov Complex. Fields: I—tholeiites, II—aluminous basalts, III—alkaline basalts.
(c) F_1 vs. F_2 component diagram for metavolcanic rocks of the Fedorov Complex. (1) Metabasalts of type I; (2) metabasalts of type II; (3) intermediate and acid metavolcanic rocks.
$F_1 = 0.895SiO_2 - 0.024TiO_2 - 0.014Al_2O_3 - 0.3FeO_t - 0.168MgO - 0.25CaO + 0.03Na_2O + 0.003K_2O$, $F_2 = -0.073SiO_2 - 0.0068TiO_2 + 0.64Al_2O_3 - 0.683FeO_t - 0.136MgO + 0.29CaO + 0.11Na_2O + 0.004K_2O$, $FeO_t = 0.9Fe_2O_3 + + FeO$ (wt %).
B is the Bowen differentiation trend (differentiation trend of the Katmai magmatic series), F is the Fenner differentiation trend (Skaergaard intrusion).

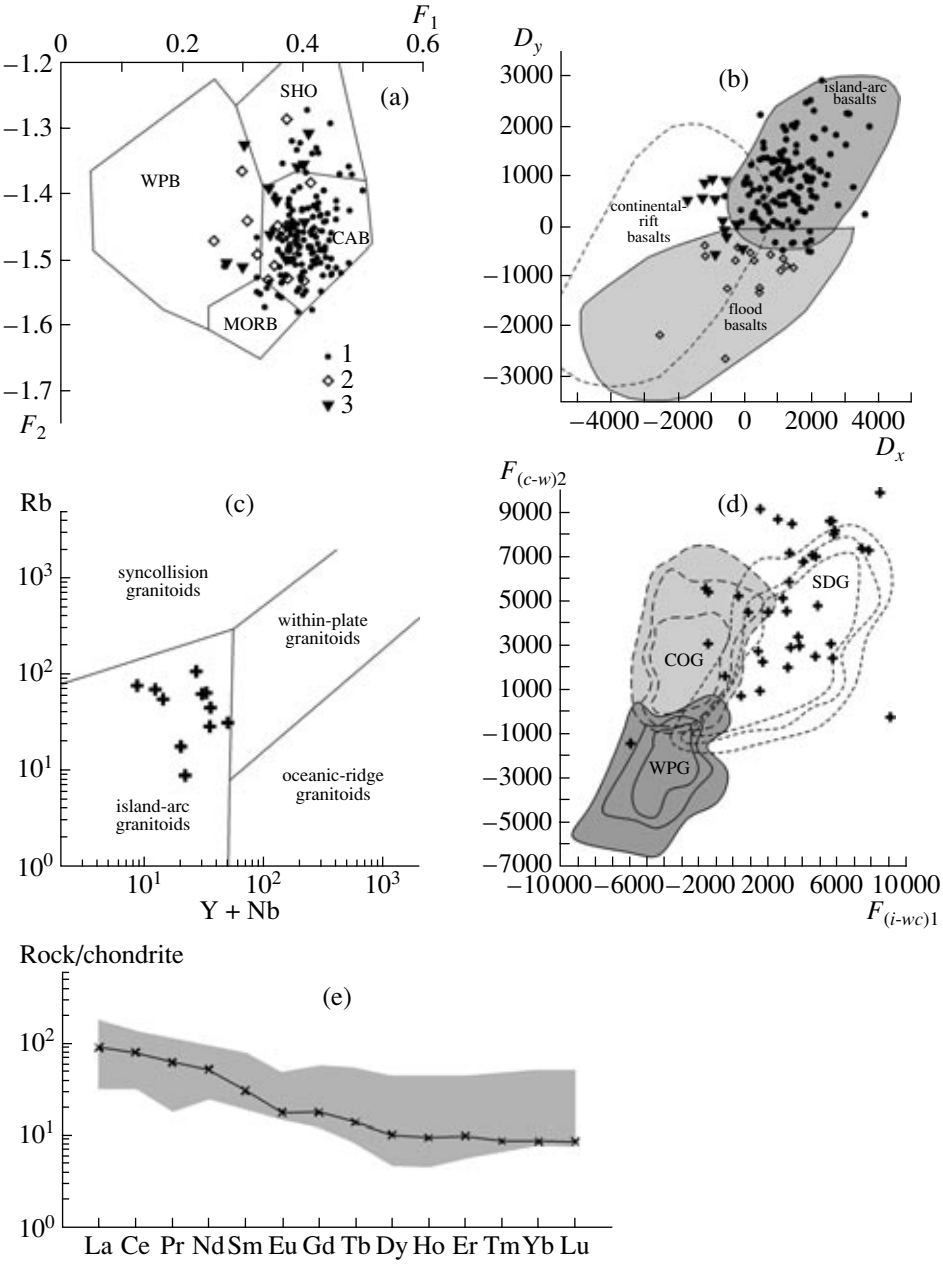

Fig. 3. Composition–tectonic setting discriminant diagrams for the metavolcanic rocks of the Fedorov Complex.

(a) F_1 vs. F_2 diagram (Pearce, 1976) for metabasalts of the Fedorov Complex. Fields: MORB—mid-oceanic ridge basalts, WPB—within-plate basalts, CAB—calc–alkaline basalts, SHO—island-arc shoshonites.

$F_1 = 0.0088SiO_2 - 0.0774TiO_2 + 0.0102Al_2O_3 + 0.0066FeO_t - 0.0017MgO - 0.0143CaO - 0.0155Na_2O - 0.0007K_2O$; $F_2 = -0.013SiO_2 - 0.0185TiO_2 - 0.0129Al_2O_3 - 0.0134FeO_t - 0.03MgO - 0.0204CaO - 0.0481Na_2O + 0.0715K_2O$.

(1) Metabasalts of type I; (2) metabasalts of type II; (3) metabasalts of type III.

(b) D_x vs. D_y diagram (Velikoslavinsky and Glebovitsky, 2005) for metabasalts of the Fedorov Complex. See Fig. 3a for symbol explanations. The contours of fields outline 95% of the data points of the basalts of the corresponding groups. The data points of island-arc basalts whose data were not taken into account when the diagram was constructed plot within the field of continental-rift basalts.

$D_x = 176.94SiO_2 - 1217.77TiO_2 + 154.51Al_2O_3 - 63.1FeO_t - 15.69MgO + 372.43CaO + 104.41Na_2O - 19.96K_2O - 873.69P_2O_5 - 11721.488$,

$D_y = 94.39SiO_2 - 103.3TiO_2 + 417.98Al_2O_3 - 55.63FeO_t + 57.61MgO + 118.42CaO + 502.02Na_2O + 6.37K_2O + 415.31P_2O_5 - 13724.66$.

(c) (Y + Nb) vs. Rb diagram (Pearce *et al.*, 1984) for salic metavolcanic rocks ($SiO_2 > 60$ wt %) of the Fedorov Complex.

(d) $F_{(i\text{-}wc)1}$ vs. $F_{(c\text{-}w)2}$ diagram (Velikoslavinsky, 2003) for salic metavolcanic rocks ($SiO_2 > 65$ wt %) of the Fedorov Complex. The diagram shows lines of the equal distribution density of the data points of within-plate (WPG), subduction (SDG), and collisional (COG) granitoids (the outer, intermediate, and inner contours outline 90, 80, and 70% of the data points, respectively).

$F_{(i\text{-}wc)1} = 2432.42SiO_2 + 7900.33TiO_2 + 2512.12Al_2O_3 + 1380.23FeO_t + 2616.55MgO + 3480.51CaO + 3045.39Na_2O + 645.91K_2O - 241285.5$,

$F_{(c\text{-}w)2} = -752.3SiO_2 - 6537.06TiO_2 - 25.6Al_2O_3 - 928.96FeO_t + 1928.07MgO - 464.21CaO - 1808.19Na_2O - 1272.16K_2O + 8675.33P_2O_5 + 71073.5$.

(e) Chondrite-normalized pattern of metadacite of the Fedorov Complex (Table 2, sample 1866). Gray field corresponds to the 95% limits of the REE concentrations in the granitoids of subduction environments (Velikoslavinsky, 2003).

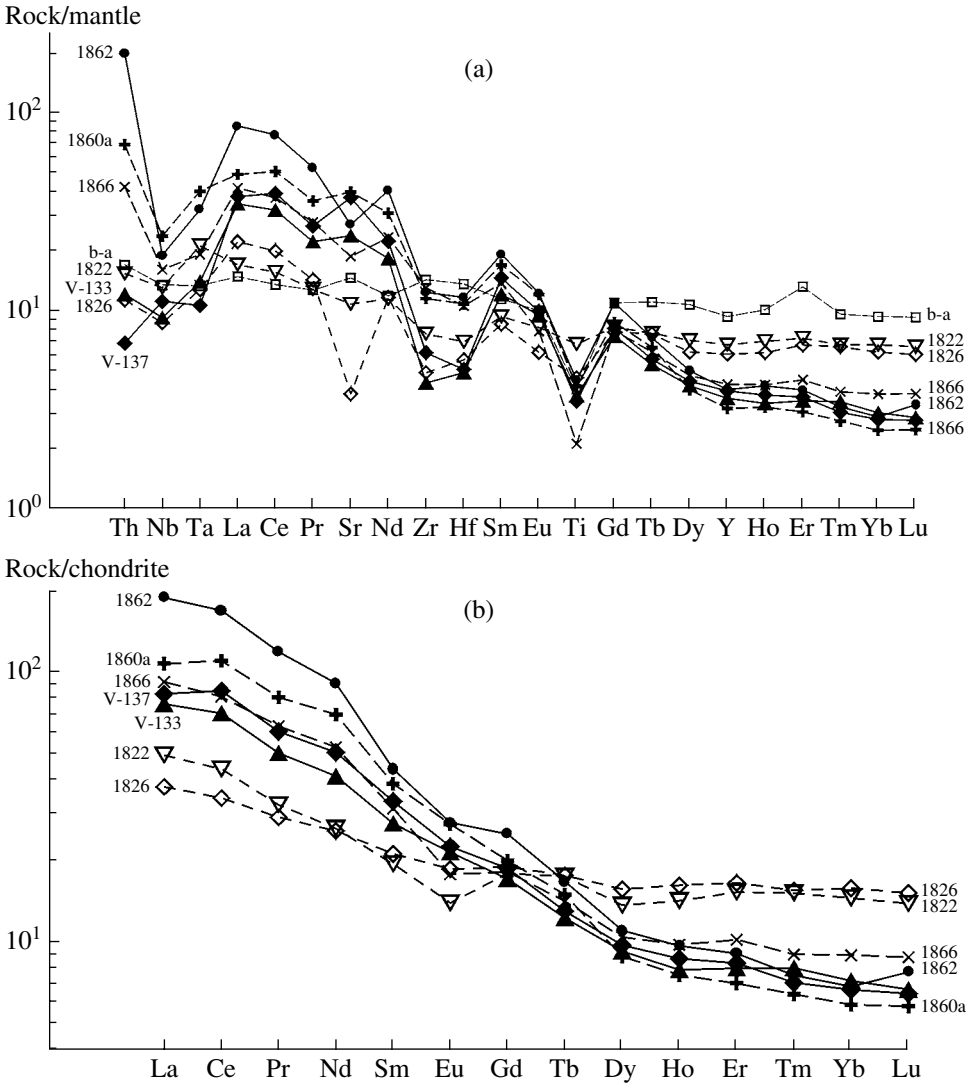

Fig. 4. Fractionation of trace elements and REE in the metavolcanic rocks of the Fedorov Complex (based on the data of Table 2).
(a) Primitive-mantle normalized (Sun and McDonough, 1989) trace-element patterns; b-a is the fractionation of trace elements in backarc basalts (Leat *et al.*, 2000).
(b) Chondrite-normalized (Taylor and McLennan, 1985) REE patterns for the metavolcanic rocks of the Fedorov Complex. See Table 1 for rock types.

absent (Eu/Eu* = 0.75–0.93). Several geochemical characteristics of these rocks are close to those of back-arc-basin basalts (Fig. 4a, pattern b–a), whose petrogenesis is participated by both depleted upper-mantle and enriched plume material (Leat *et al.*, 2000). At the same time, the poorly pronounced Nb–Ta anomaly (Fig. 4a) makes the type-II metabasalts similar to continental flood basalts and basalts in rift zones within active continental margins (Condie, 1997, 2001; Kerr *et al.*, 2000).

Hypersthene gneisses. The hypersthene gneisses are characterized by broad compositional variations. For example, their concentrations of silica vary from 53 to 77 wt % (Table 1). The chemical composition of these rocks corresponds to that of basaltic andesites, andesites, dacites, and rhyolites of the subalkaline or, more rarely, normal and alkaline series (Table 1; *Early Precambrian…*, 1986; Velikoslavinsky *et al.*, 1990, 1993).

These is still no consensus on the character of the protoliths of the Fedorov gneisses. The currently prevailing viewpoint is that these rocks were produced by the quasi-isochemical metamorphism of volcanic–sedimentary rocks (Reutov, 1981) or intermediate and acid volcanics (*Early Precambrian…*, 1986). At the same time, many researchers believe that at least some of the Fedorov gneisses were formed by means of migmatization (charnockitization and enderbitization) of mafic schists (Belyaev and Rudnik, 1978). Materials available for the authors of this publication confirm the con-

cept that the protoliths of the Fedorov gneisses were volcanic rocks. This is evident from the following data:

(i) The chemical compositions of most hypersthene gneisses from different stratigraphic units of the Aldan granulite–gneiss megacomplex, including the Fedorov Complex, correspond to those of orthorocks (Fig. 5).

(ii) The petrochemical variability of the Fedorov hypersthene gneisses corresponds to the Bowen differentiation trend. The differentiation trend of the intermediate and acid metavolcanic rocks is a continuation of the differentiation trend of the type-I high-Al metabasalts (Fig. 2c), which makes it possible to regard the protoliths of the Fedorov mafic schists and hypersthene gneisses as components of a single continuous differentiated series.

(iii) The discriminant analysis of the concentrations of major and trace elements in hypersthene gneisses from the main stratigraphic units of the Aldan granulite–gneiss megacomplex demonstrates that the gneisses of the Kurumkan Complex, Fedorov Complex, Kholbolokh association, Kyurikan Complex, and Idzhek Complex, which are often grouped into the Timpton–Dzheltula Complex, and the mafic schists of these stratigraphic units significantly differ in composition (Velikoslavinsky, 1998). This stratigraphic control suggests a volcanic (volcanic sheets and subvolcanic sills) but not intrusive nature of the protoliths.

The Fedorov hypersthene gneisses are characterized by the distribution of trace elements and REE similar to those of the type-I metabasalts (Table 2, Fig. 4). The rocks have well-pronounced negative anomalies at Nb, Ta (La/Nb = 2.0–2.5), Zr, Hf, and Ti (Fig. 3a), moderately fractionated REE [$(La/Yb)_N$ = 10.3–18.4], and fractionated LREE and HREE [$(La/Sm)_N$ = 2.8–2.9, $(Gd/Yb)_N$ = 2.0–3.4; Fig. 4b). The succession basaltic andesite–andesite–dacite–rhyolite displays no systematic variations in the contents of REE. These geochemical characteristics suggest that the type-I metabasalts (high-Al metabasalts) are petrogenetically similar to the intermediate–acid metavolcanics of the Fedorov Complex.

In discrimination tectonic diagrams (Figs. 3c, 3d), the data points of the hypersthene gneisses (salic metavolcanics) of the Fedorov Complex plot within the field of granitoids from subduction environments. The REE patterns of the acid metavolcanics of the Fedorov Complex correspond to those of granitoids from subduction environments.

U–Pb GEOCHRONOLOGY

The U–Pb geochronologic study was conducted on sample 1857 of melanocratic quartz-bearing hypersthene–biotite–hornblende plagioclase gneiss (metamorphosed basaltic andesite, more specifically, metamorphosed trachybasaltic andesite) from the Fedorov Complex, sampled in a riverbank exposure at the Timpton River (Fig. 1, no. 4).

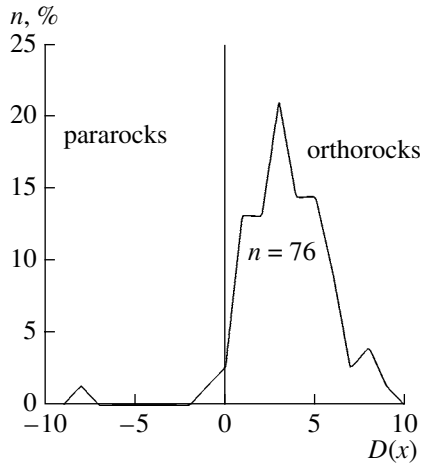

Fig. 5. Distribution of the values of the function $D(x)$ (Shaw, 1972) discriminating between ortho- and pararocks of intermediate and acid composition. The values are calculated for the gneisses of the Fedorov Complex.

The accessory zircon separated from this sample consists of transparent and semitransparent subhedral crystals of prismatic and short-prismatic habit and pale pink color (Figs. 6a–6d). The faceting of the crystals is determined by various combinations of prisms {100} and {110} and dipyramids {111}, {011}, and {101}. The cores of most crystals are usually transparent, weakly fissured and display zoning (Figs. 6e–6k). In addition, the cores of some short-prismatic crystals have sectorial zoning (Figs. 6e, 6j, 6k). The outermost zones of the crystals are fractured, have lower birefringence, and partly loose their magmatic zoning (Figs. 8e, 8h–8j). The crystals range from 50 to 300 μm, K_{el} = 1.6–2.5.

The U–Pb study was originally conducted on two batches of the most transparent zircon crystals selected from the size fractions –85+60 μm and –150+100 μm, which appeared to be notably discordant (Table 3, Fig. 7, nos. 1, 2). In order to reduce the discordance, we air-abraded 20 zircon grains from the fraction –150+100 μm (Table 3, no. 3) and treated zircon from the fraction >85 μm by acid for 2 h (Table 3, no. 4). As can be seen from Fig. 9, the isotopic composition point of the acid-leached zircon residue lies on the concordia, and its $^{207}Pb/^{206}Pb$ age is equal to 2004 ± 1 Ma. The data points of all other analyzed zircon fractions define a regression line whose upper intercept with the concordia corresponds to an age of 2006 ± 3 Ma, and the lower intercept corresponds to an age of 328 ± 10 Ma (MSWD = 0.49). The morphology of the zircon indicates that it is of magmatic provenance, and, hence, there are good reasons to believe that the aforementioned age estimate of 2006 ± 3 Ma corresponds to the crystallization age of the protolith of the metamorphosed basaltic andesites of the Fedorov Complex.

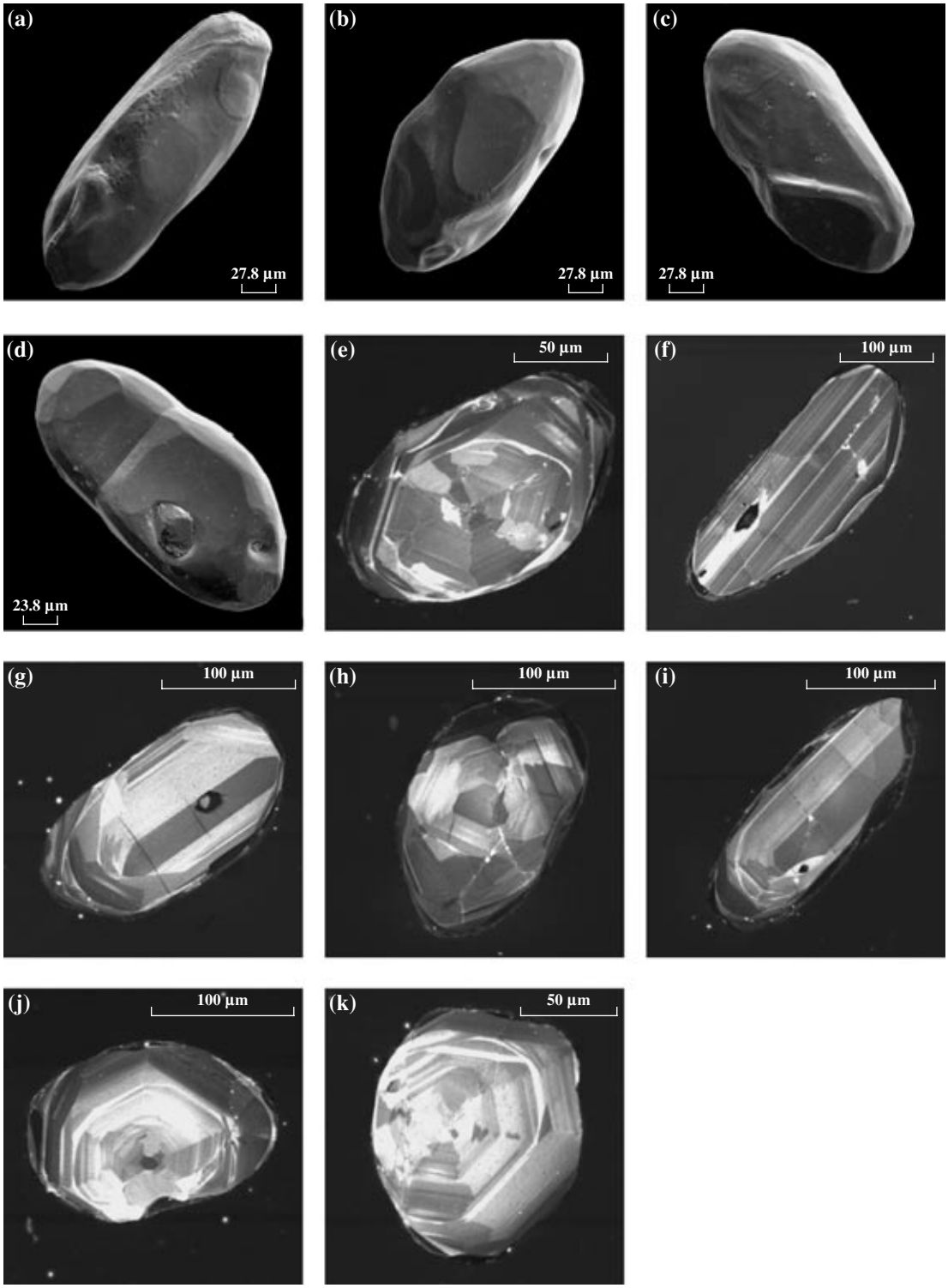

Fig. 6. SEM images of zircon crystals from hypersthene–hornblende plagioclase gneiss (metaandesites) of the Fedorov Complex (sample 1857).
(a–d) ABT-55 scanning electron microscope (accelerating voltage 20 kV); (e–k) Centaurus cathodoluminescence detector, CamScan scanning electron microscope (accelerating voltage 15 kV).

Sm–Nd ISOTOPIC STUDY

The Sm–Nd isotopic study was conducted on samples of the mafic schists whose chemical composition and REE patterns correspond to the metabasalts of type I (Table 4, no. 1) and type II (Table 4, nos. 2–4); hypersthene gneisses of andesite–rhyolite composition (Table 4, nos. 5–11); and hypersthene–hornblende pla-

Table 3. U–Pb isotopic data on zircon from hypersthene–hornblende plagioclase gneiss (metamorphosed basaltic andesite) from the Fedorov Complex (sample 1857)

no.	Size fraction (μm) and its characteristics	Sample (mg)	Concentration (ppm)		Isotopic ratios		
			Pb	U	$^{206}Pb/^{204}Pb$	$^{207}Pb/^{206}Pb^a$	$^{208}Pb/^{206}Pb^a$
1	–85+60	1.32	78.4	325	4822	0.1161 ± 1	0.1099 ± 1
2	–150+100	0.64	58.6	229	3415	0.1172 ± 1	0.1155 ± 1
3	–150+100, A 60%, 20 grains	0.15	13.2	35.8	395	0.1212 ± 4	0.1690 ± 1
4	>85, ISR	–	U/Pb* = 2.4		8901	0.1233 ± 1	0.1939 ± 1

no.	Size fraction (μm) and its characteristics	Isotopic ratios		Rho	Age (Ma)		
		$^{207}Pb/^{235}U$	$^{206}Pb/^{238}U$		$^{207}Pb/^{235}U$	$^{206}Pb/^{238}U$	$^{207}Pb/^{206}Pb$
1	–85+60	3.6242 ± 72	0.2264 ± 5	0.97	1555 ± 3	1315 ± 3	1897 ± 0.6
2	–150+100	3.8529 ± 77	0.2384 ± 5	0.96	1604 ± 3	1378 ± 3	1914 ± 0.7
3	–150+100, A 60%, 20 grains	5.1902 ± 228	0.3104 ± 10	0.58	1851 ± 8	1743 ± 6	1975 ± 6.4
4	>85, ISR	6.1613 ± 123	0.3625 ± 7	0.96	1999 ± 4	1994 ± 4	2004 ± 0.6

Note: [a] The isotopic ratios are corrected for the blank and common Pb; A 60% means that 60% of the zircon material was removed by air abrasion; ISR insoluble residue after acid treatment; * zircon sample was not determined; Rho is the correlation coefficient of errors in the determined $^{206}Pb/^{238}U$ and $^{207}Pb/^{236}U$ ratios. The errors (2σ) correspond to the last decimal digits.

gioclase gneisses (Table 4, no. 12), whose composition corresponds to graywacke. Most of the rocks were sampled in the middle reaches of the Timpton River (Fig. 1), near the stratotype of the Fedorov Complex (the Fedorov group of phlogopite deposits). In contrast to the stratotype, the rocks of the Fedorov Complex in this area are practically not affected by Mg–Fe–Ca metasomatism, i.e., they are the most suitable for isotopic–geochronologic studies.

As follows from Table 4, the Fedorov volcanic rocks can be subdivided into two groups according to their Nd isotopic composition. The first group comprises mafic schists (metabasalts of type I) and hypersthene plagioclase gneisses, which are analogues of volcanic rocks of the differentiated subalkaline basalt–andesite–dacite–rhyolite series of the island-arc type. The rocks of this group have $\varepsilon_{Nd}(T)$ from –0.1 to +3.1 and Nd model ages $T_{Nd}(DM)$ of 2.2–2.4 Ga. The values of the two-stage Nd model age $T_{Nd}(DM\text{-}2st)$ coincide with the single-stage ages (Table 4), a fact testifying to the absence of Sm and Nd fractionation during any overprinted high-temperature metamorphic alterations. Similar Nd model ages $T_{Nd}(DM) = T_{Nd}(DM\text{-}2st) = 2.2$ Ga were yielded by the hypersthene–hornblende plagioclase gneisses (metagraywackes) of the Fedorov Complex.

The mafic schists of group II (type-II metabasalts), whose chemical compositions are comparable with those of continental basalts, have elevated $^{147}Sm/^{144}Nd$ = 0.1444–0.1599 and negative $\varepsilon_{Nd}(T)$ from –2.1 to –5.4. Geochemical and isotopic data indicate that the sources of the parental melts of the type-II metabasalts could be the rocks of the enriched mantle with minor amounts of crustal material.

DISCUSSION

Currently available data indicate that the protoliths of the gneisses and mafic schists of the Fedorov Complex consisted mostly of acid, intermediate, and mafic

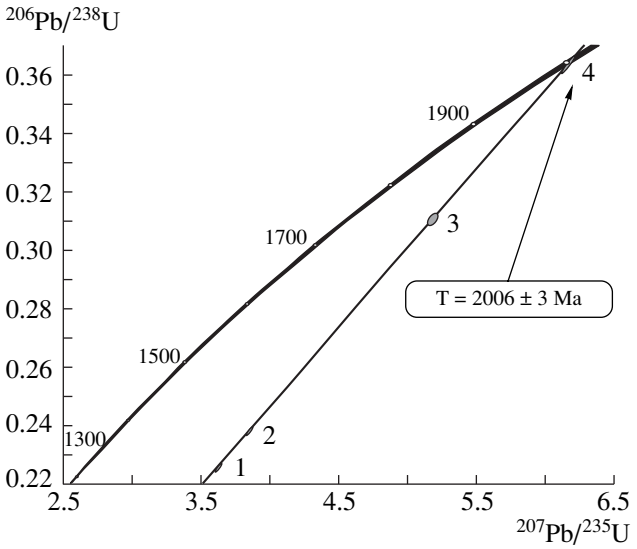

Fig. 7. Concordia diagram for zircon from hypersthene–hornblende plagioclase gneiss (metamorphosed basaltic andesite) of the Fedorov Complex (sample 1857).

Table 4. Sm–Nd isotopic data on metamorphic rocks from the Fedorov Complex

no.	Sample	Sm, ppm	Nd, ppm	$^{147}Sm/^{144}Nd$	$^{143}Nd/^{144}Nd$ ($\pm 2\sigma_{meas}$)	$\varepsilon_{Nd}(0)$	$\varepsilon_{Nd}(T)$	$T_{Nd}(DM)$, Ma	$T_{Nd}(DM\text{-}2st)$, Ma
1	1862	8.86	57.6	0.0933	0.511269 ± 9	−26.7	−0.1	2373	2478
2	V-132	4.05	15.37	0.1599	0.512045 ± 10	−11.6	−2.1		
3	1822	4.03	15.4	0.1586	0.511996 ± 13	−12.5	−2.7		
4	1826	3.62	15.21	0.1444	0.511669 ± 11	−18.9	−5.4		
5	1857	8.80	48.2	0.1103	0.511513 ± 4	−21.9	0.3	2371	2433
6	1860a	7.19	41.9	0.1040	0.511438 ± 5	−23.4	0.5	2252	2264
7	1890	7.58	39.9	0.1153	0.511693 ± 7	−18.4	2.5	2375	2411
8	1866	6.22	34.0	0.1110	0.511544 ± 14	−21.3	0.8	2261	2333
9	1908b	1.42	9.18	0.0937	0.511365 ± 5	−24.8	1.7	2158	2216
10	1907a	2.37	17.06	0.0843	0.511313 ± 4	−25.8	3.1	2313	2390
11	1880g	1.92	12.07	0.0966	0.511367 ± 5	−24.8	1.0	2313	2390
12	B-2880/1	3.38	17.22	0.1192	0.511776 ± 5	−16.8	3.2	2211	2213

Note: See note to Table 1 for brief characteristics of the samples. The values of $\varepsilon_{Nd}(T)$ and $T_{Nd}(DM\text{-}2st)$ were calculated for an age of 2006 Ma.

volcanic rocks: rhyolites, dacites, andesites, and basaltic andesites, mostly of normal alkalinity, as well as subalkaline and alkaline basalts. The Fedorov Complex contains obviously subordinate amounts of paragneisses (metagraywackes) (Fig. 5; *Early Precambrian…*, 1986).

Judging from geochemical data, the metavolcanic rocks of the Fedorov Complex consist of three petrographic groups (Fig. 3b): (i) volumetrically predominant (at least 90% of the complex by volume, according to provisional estimates) rocks of a continuous differentiated island-arc basalt–andesite–dacite–rhyolite series (Fig. 2); (ii) within-plate basalts, which are dominated by basalts of composition similar to those of low-Ti flood basalts; (iii) subordinate amounts of varieties close to continental-rift basalts. This can lead to the conclusion that the Fedorov Complex was produced in a subduction environment. The alkaline and subalkaline composition of the metavolcanic rocks and the wide occurrence of the acid metavolcanics justifies the comparison of the Fedorov Complex with the volcanic complexes of Phanerozoic ensialic island arcs or continental margins. Now there are no geological evidence that the distinguished geochemical groups of metabasalts of the Fedorov Complex differ in age. Because of this, the tectonic setting of the within-plate metabasalts is still not fully understood. Conceivably, their genesis can be related to rifting following after or coeval with the subduction processes (for example, continental rifting corresponding to the initial evolutionary stages of a backarc basin) and/or the superposition of a hotspot.

Our U–Pb dates of the rocks completely corroborate the earlier conclusion (drawn from Sm–Nd isotopic data) that the Fedorov Complex of the Aldan granulite–gneiss megacomplex has an Early Proterozoic age (Kovach *et al.*, 1996a, 1999), which, in turn, calls for the revision of the corresponding stratigraphic schemes for the Precambrian of the Aldan Shield. The upper age limit of the Fedorov Complex is constrained by the age of the subalkaline and quartz diorites that intrude it (1993 ± 1 Ma; Kotov *et al.*, 1995a) and that were emplaced during the granulite-facies metamorphic culmination (Kotov and Samorukova, 1990).

At the same time, the structural transformations related to the development of the Fedorov Allochthon affected, along with the rocks of the Fedorov Complex itself, also the biotite–hypersthene tonalite–trondhjemite orthogneisses and granite-gneisses of the Timpton Complex, which are sometimes interpreted (*Earlier Precambrian…*, 1986) as the unstratified infracrustal complex in the eastern part of the Nimnyr block of the Aldan Shield, which is the basement of the Fedorov Complex. Available data (Velikoslavinsky *et al.*, 2003) indicate that the granites shown in Fig. 1 as composing the Timpton Complex were formed in different (subduction and collisional) tectonic environments, which implies their polygenetic and polychronous nature. The protolith age of the tonalite–trondhjemite orthogneisses of the Timpton Complex is 2011 ± 2 Ma (Kotov *et al.*, 1995a) and suggests the origin of these rocks in relation to the subduction processes that also produced the Fedorov Complex.

If these concepts prove valid, the overall time span during which the Fedorov Complex was formed seems to have been no more than 25 m.y. The origin of collisional granite-gneisses that are spatially combined with subduction-related rocks was likely caused by subsequent collision events.

The Nd isotopic data obtained on metavolcanic rocks of the Fedorov Complex, namely, their Nd model ages $T_{Nd}(DM)$ = 2.2–2.4 Ga, which are close to the crystallization age, as well as $\varepsilon_{Nd}(T)$ from –0.1 to + 3.1, which are close to zero or positive, are in good agreement with the model of the origin of the parental melts of these rocks in a subduction environment as a result of the melting of a depleted mantle source with an insignificant amount of ancient crustal material. In light of these data, the genesis of the metavolcanics of the Fedorov Complex reflects the processes of the origin of the Early Proterozoic continental crust. The source of the ancient crustal material was most probably the orthogneisses of the Aldan Complex with $T_{Nd}(DM)$ = 3.0–3.9 Ga and $\varepsilon_{Nd}(2.0)$ from –10.8 to –18.4 (Kotov *et al.*, 1995a; Sal'nikova *et al.*, 1996) and/or the metamorphic rocks of the Kurumkan and Amedichi complexes with $T_{Nd}(DM)$ = 3.0–3.8 Ga (Kovach *et al.*, 1996b; Kotov, 2003). The remelting of the erosion products of these rocks in the subduction zone was responsible for the $\varepsilon_{Nd}(T)$ values of the Fedorov Complex lower than those of the depleted mantle and caused the insignificant overestimation of their Nd model age relative to the crystallization age.

It is worth noting the fact that the estimate of the protolith age (2006 ± 3 Ma) of the Fedorov metamorphosed basaltic andesites coincides with the evaluated age of the tonalite–trondhjemite orthogneisses of the Timpton Complex (2011 ± 2 Ma; Kotov *et al.*, 1995) and the Ungra gabbro–diorite–tonalite–trondhjemite complex (2016 ± 5 Ma; Kotov *et al.*, 2003), which were most probably formed in the environment of an active continental margin (Kotov, 2003). This makes it possible to consider the genesis of the Fedorov and aforementioned complexes within the framework of the geodynamic system of an active continental margin of the Olekma–Aldan continental microplate and the Fedorov island arc.

In general, with regard for all currently available geological, geochronological, and isotopic geochemical data (Bibikova *et al.*, 1986; Kotov *et al.*, 1993, 1995a, 2004; Kovach *et al.*, 1996a, 1996b, 1999; Kotov, 2003; Sal'nikova *et al.*, 1996; Frost *et al.*, 1998), the following provisional scheme can be proposed for the geologic evolution of the western part of the Aldan geoblock in the Early Proterozoic:

1.99–2.01 Ga. Origin of the geodynamic system of the eastern active margin of the Olekma–Aldan continental plate and the Fedorov island arc and the related accumulation of the sedimentary–volcanic deposits of the Fedorov Complex (2006 ± 3 Ma), the emplacement of polyphase gabbro–diorite–tonalite–trondhjemite intrusions of the Ungra Complex (2016 ± 5 Ma; Kotov *et al.*, 2003), and the origin of the protoliths of the tonalite–trondhjemite orthogneisses of the Timpton Complex (2011 ± 2 Ma; Kotov *et al.*, 1995). The accumulation of sedimentary–volcanic deposits of the Chuga Complex of the Aldan granulite–gneiss megacomplex on the continental margin. The accretion of the Fedorov island arc to the Olekma–Aldan continental microplate, and the development of deep-seated plastic overthrusts of the Fedorov system (Fedorov allochthon). The emplacement of syntectonic intrusions of subalkaline quartz diorite and subalkaline diorites (1993 ± 1 Ma; Kotov *et al.*, 1995a).

1.95–1.97 Ga. Emplacement of late-collision (relative to the collision between the Fedorov island arc and the Olekma–Aldan continental microplate) intrusions of biotite and amphibole–biotite granites, subalkaline granites, and leucogranites of the Dzhaltunda Complex (1966 ± 4 Ma; Kotov *et al.*, 2004) and hypersthene-bearing granites and subalkaline granites exposed in the middle reaches of the Seimd'e River (1950 ± 2 Ma; Kotov, 2003).

1.92–1.95 Ga. The accumulation of sedimentary–volcanic deposits of the Idzhek and Kyurikan complexes of the Aldan granulite–gneiss megacomplex in a subduction environment, on the active margin of the Olekma–Aldan continental microplate (Kotov, 2003). Collision of the Olekma–Aldan continental microplate and the passive margin of the Uchur continental microplate (formation of the Aldan continental plate). Origin of the Timpton deep plastic overthrust, faults of the Amga system, and the major mappable northwest-trending and submeridional linear folds of the Aldan geoblock. Emplacement of intrusions of biotite–hypersthene–amphibole quartz diorites and tonalites (1925 ± 5 Ma; Kotov, 2003). Origin of the protoliths of the hypersthene–biotite tonalite–trondhjemite orthogneisses (1918 ± 1 Ma; Frost *et al.*, 1998).

1.89–1.92 Ga. Emplacement of postorogenic intrusions of the Amut Complex (1899 ± 6 Ma; Kotov *et al.*, 2004) and its coeval and coeval–structural analogues: biotite granites (1901 ± 1 Ma; Frost *et al.*, 1998), leucogranites (1907 ± 15 Ma; Kotov *et al.*, 1993), and charnockites of the Ust'-Idzhek Massif (1916 ± 10 Ma; Bibikova *et al.*, 1986).

CONCLUSIONS

The materials presented in this publication led us to the following conclusions:

(1) The Fedorov Complex is dominated by metavolcanic rocks of a differentiated basalt–andesite–dacite–rhyolite series. The crystallization age of the protoliths of the metamorphosed basaltic andesites of this complex is 2006 ± 3 Ma, and the series was produced over a time span of 25 m.y.

(2) The volcanic rocks of the Fedorov Complex were formed in a subduction environment (ensialic

island arc). An insignificant part of the protolithic rocks of the Fedorov metabasalts that have "within-plate" geochemical signatures could be produced during synchronous subduction or subsequent rifting.

ACKNOWLEDGMENTS

This study was supported by the Russian Foundation for Basic Research (project nos. 00-05-72011, 01-05-65266, 02-05-64209, 02-05-65086, and 04-05-64810), NSH-615.2003.05, Fundamental-Research Programs "The Geodynamic Evolution of the Lithosphere in the Central Asian Foldbelt: From Paleocean to Continent" and "Isotopic Geology: Geochronology and Material Sources" of the Division of Earth Sciences, Russian Academy of Sciences, and by the Foundations for the Support of National Science.

REFERENCES

1. G. M. Belyaev and V. A. Rudnik, *Formational–Genetic Types of Granitoids* (Nedra, Leningrad, 1978) [in Russian].
2. E. V. Bibikova, G. M. Drugova, V. L. Duk, *et al.*, "The Geochronology of the Aldan–Vitim Schield," in *Methods of Isotopic Geology and the Geochronological Scale* (Nauka, Moscow, 1986), pp. 135–139 [in Russian].
3. K. C. Condie, *Mantle Plumes and Their Records in Earth History* (Cambridge University Press, Cambridge, 2001).
4. K. C. Condie, *Plate Tectonic and Crustal Evolution* (Butterworth-Heinemann, London, 1997).
5. V. L. Duk, "Stages of Nappe Formation in the Central Part of the Aldan Granulite–Gneiss Terrain," in *Abstracts of Papers of the V All-Russian Conference "Structural Analysis of Crystalline Complexes"* (Vseross. Geol. Inst., St. Petersburg, 1994), pp. 19–20 [in Russian].
6. V. L. Duk, M. E. Sal'e, and V. S. Baikova, *The Granulites of the Aldan Area: Structural–Metamorphic Evolution and Phlogopite-Bearing Potential* (Nauka, Leningrad, 1975) [in Russian].
7. Yu. K. Dzevanovskii, "The Aldan Shield," in *The Geological Structure of USSR* (Geol. Okhrana Nedr, Moscow, 1958), Vol. 3, pp. 48–50 [in Russian].
8. *The Early Precambrian of Southern Yakutia*, Ed. by N. L. Dobretsov (Nauka, Moscow, 1986) [in Russian].
9. B. R. Frost, O. V. Avchenko, K. R. Chamberlain, and C. D. Frost, "Evidence for Extensive Proterozoic Remobilization of the Aldan Shield and Implications for Proterozoic Plate Tectonic Reconstructions of Siberia and Laurentia," Precambrian Res. **89**, 1–23 (1998).
10. *An 1 : 3,000,000-Scale Geological Map of the BAM Territory*, Ed. by L. I. Krasnyi (Vsess. Geol. Inst., Leningrad, 1988) [in Russian].
11. S. J. Goldstein and S. B. Jacobsen, "Nd and Sr Isotopic Systematics of River Water Suspended Material: Implications for Crustal Evolution," Earth Planet. Sci. Lett. **87** (3), 249–265 (1988).
12. S. B. Jacobsen and G. J. Wasserburg, "Sm–Nd Evolution of Chondrites and Achondrites," Earth Planet. Sci. Lett. **67**, 137–150 (1984).
13. A. C. Kerr, R. V. White, and A. D. Saunders, "LIP Reading: Recognizing Oceanic Plateaux in the Geological Record," J. Petrol. **41**, 1041–1056 (2000).
14. D. S. Korzhinskii, *Petrology of the Archean of the Aldan Plate* (ONTI, Leningrad, 1936) [in Russian].
15. A. B. Kotov and L. M. Samorukova, *The Evolution of Granite Formation in Early Precambrian Tectonic–Metamorphic Cycles* (Nauka, Leningrad, 1990) [in Russian].
16. A. B. Kotov, E. B. Sal'nikova, A. M. Larin, *et al.*, "Early Proterozoic Granitoids in the Junction Zone of the Olekma Granite–Greenstone Belt and the Aldan Granulite–Gneiss Terrane, Aldan Shield: Age, Sources, and Geodynamic Environments," Petrologiya **12** (1), 46–67 (2004) [Petrology **12** (1), 37–55 (2004)].
17. A. B. Kotov, V. P. Kovach, E. B. Sal'nikova, *et al.*, "The Evolution of the Continental Crust in the Central Aldan Granulite–Gneiss Terrane," Petrologiya **3** (1), 99–110 (1995a).
18. A. B. Kotov, Extended Abstract of Doctoral Dissertation in Geology and Mineralogy (St. Petersburg Gos. Univ., St. Petersburg, 2003).
19. A. B. Kotov, I. M. Morozova, E. B. Sal'nikova, *et al.*, "Early Proterozoic Granitoids in the Northwestern Aldan Granulite–Gneiss Terrane," Geol. Geofiz. **34** (2), 15–21 (1993).
20. A. B. Kotov, V. M. Shemyakin, E. B. Sal'nikova, and V. P. Kovach, "Formation Stages and Isotope Structure of the Continental Crust of the Sutam Block, Aldan Shield: Evidence from Sm–Nd Isotope Systematics of Granitoids," Dokl. Akad. Nauk **366** (6), 809–812 (1999) [Dokl. Earth Sci. **367** (5), 695–697 (1999)].
21. A. B. Kotov, E. B. Sal'nikova, S. Z. Yakovleva, *et al.*, "Formation Age Limits of Early Nappes in the Central Part of Aldan Granulite–Gneiss Terrane," Dokl. Akad. Nauk **342** (2), 209–212 (1995b).
22. V. P. Kovach, A. B. Kotov, A. P. Smelov, *et al.*, "Evolutionary Stages of the Continental Crust in the Buried Basement of the Eastern Siberian Platform: Sm–Nd Isotopic Data," Petrologiya **8** (4), 394–408 (2000) [Petrology **8** (4), 353–365 (2000)].
23. V. P. Kovach, S. D. Velikoslavinsky, A. B. Kotov, and E. B. Sal'nikova, "Sm–Nd Isotopic Systematics of the Acid Metavolcanites of the Fedorov Group in the Aldan Shield (Middle Reaches of the Timpton River)," Dokl. Akad. Nauk **347** (2), 236–238 (1996a) [Dokl. Earth Sci. **347** (2), 345–347 (1996a)].
24. V. P. Kovach, A. B. Kotov, V. I. Berezkin, *et al.*, "Age Limits of High-Grade Metamorphic Supracrustal Complexes in the Central Aldan Shield: Sm–Nd Isotopic Data," Stratigr. Geol. Korrel. **7** (1), 3–17 (1999) [Stratigr. Geol. Correl. **7** (1), 1–15 (1999)].
25. V. P. Kovach, A. B. Kotov, E. B. Sal'nikova, *et al.*, "Sm–Nd Isotopic Systematics of the Kurumkan Subgroup, the Iengra Group of Aldan Shield," Stratigr. Geol. Korrel. **4** (3), 3–10 (1996b) [Stratigr. Geol. Correl. **4** (3), 213–220 (1996b)].
26. T. E. Krogh, "A Low Contamination Method for Hydrothermal Composition of Zircon and Extraction of U and Pb for Isotopic Age Determination," Geochim. Cosmochim. Acta **37**, 485–494 (1973).
27. H. Kuno, "High Alumina Basalt," J. Petrol. **1**, 121–145 (1961).

28. A. M. Larin, A. B. Kotov, E. B. Sal'nikova, *et al.*, "New Data on the Age of Granites of the Kodar and Tukuringra Complexes, Eastern Siberia: Geodynamic Constraints," Petrologiya **8** (3), 267–279 (2000) [Petrology **8** (3), 238–248 (2000)].
29. A. M. Larin, A. B. Kotov, E. B. Sal'nikova, *et al.*, "Age of the Katugin Ta–Nb Deposit, Aldan–Stanovoi Shield: Evidence for the Identification of the Global Rare Metal Metallogenic Epoch," Dokl. Akad. Nauk **383** (6), 807–811 (2002) [Dokl. Earth Sci. **383A** (3), 336–340 (2002)].
30. P. T. Leat, R. A. Livermore, I. L. Millar, and J. A. Pearce, "Magma Supply on Back-Arc Spreading Centre Segment E2, East Scotia Ridge," J. Petrol. **41**, 845–866 (2000).
31. T. C. Liew and A. W. Hofmann, "Precambrian Crustal Components, Plutonic Associations, Plate Environment of the Hercynian Fold Belt of Central Europe: Indications from Nd and Sr Isotopic Study," Contrib. Mineral. Petrol. **98**, 129–138 (1988).
32. K. R. Ludwig, "PbDat for MS-DOS, Version 1.21," US Geol. Surv. Open-File Rept., 88-542 (1991).
33. K. R. Ludwig, "ISOPLOT/Ex. Version 2.06: A Geochronological Toolkit for Microsoft Excel," Berkley Geochronology Center, Spec. Publ. 1a (1999).
34. *Magmatic Rocks: Classification, Nomenclature, and Petrography* (Nauka, Moscow, 1983), Part 1 [in Russian].
35. J. M. Mattinson, "A Study of Complex Discordance in Zircons Using Step-Wise Dissolution Techniques," Contrib. Mineral. Petrol. **116**, 117–129 (1994).
36. L. A. Neymark, V. P. Kovach, A. A. Nemchin, *et al.*, "Late Archean Intrusive Complexes in the Olekma Granite–Greenstone Terrain (Eastern Siberia): Geochemical and Isotopic Study," Precambrian Res. **62**, 453–472 (1993).
37. A. P. Nutman, I. V. Chernyshev, H. Baadsgaard, and A. P. Smelov, "The Aldan Shield of Siberia, USSR: The Age of Its Archean Components and Evidence for Widespread Reworking in the Mid-Proterozoic," Precambrian Res. **54**, 195–210 (1992).
38. J. A. Pearce, "Major Element Patterns in Basalts," J. Petrol. **17** (1), 15–43 (1976).
39. J. A. Pearce, N. B. W. Harris, and A. G. Tindle, "Trace Element Discrimination Diagrams for the Interpretation of Granitic Rocks," J. Petrol. **25** (4), 956–983 (1984).
40. Z. I. Petrova and V. I. Levitskii, "Basic Crystalline Schists in Eastern Siberian Granulite–Gneiss Terranes and Their Protoliths," in *Geochemistry of Volcanics in Different Geodynamic Environments* (Nauka, Novosibirsk, 1986), pp. 18–34 [in Russian].
41. Z. I. Petrova, L. K. Pozharitskaya, V. M. Roizenman, *et al.*, *The Metamorphic Complex of Aldan Phlogopite Deposits* (Nauka, Novosibirsk, 1975) [in Russian].
42. *Precambrian Geology of the USSR*, Ed. by D. V. Rundkvist and F. P. Mitrofanov (Nauka, Leningrad, 1988) [in Russian].
43. L. M. Reutov, *The Precambrian of the Central Aldan* (Nauka, Novosibirsk, 1981) [in Russian].
44. V. A. Rudnik, *Precambrian Granite and Crustal Growth* (Nedra, Leningrad, 1975) [in Russian].
45. E. B. Sal'nikova, A. B. Kotov, A. A. Nemchin, *et al.*, "The Age of the Tungurchakan Massif, Olekma Granite–Greenstone Terrain, Aldan Shield," Dokl. Akad. Nauk **331** (3), 356–358 (1993).
46. E. B. Sal'nikova, A. B. Kotov, B. V. Belyatskii, *et al.*, "U–Pb Age of Granitoids in the Junction Zone between the Olekma Granite–Greenstone and Aldan Granulite–Gneiss Terrains," Stratigr. Geol. Korrel. **5** (2), 3–12 (1997) [Stratigr. Geol. Correl. **5** (2), 101–109 (1997)].
47. E. B. Sal'nikova, V. P. Kovach, A. B. Kotov, and A. A. Nemchin, "Evolution of the Continental Crust in the Western Aldan Shield: Evidence from the Sm–Nd Systematics of Granitoids," Petrologiya **4** (2), 78–93 (1996) [Petrology **4** (2), 105–118 (1996)].
48. L. I. Salop and L. V. Travin, "New Stratigraphic Data for the Archean of the Central Aldan Shield," in *Problems in the Geology of Siberian Platform and Its Frame* (Vsess. Geol. Inst., Leningrad, 1974), pp. 5–82 [in Russian].
49. D. M. Shaw, "The Origin of the Apsley Gneisses, Ontario," Can. J. Earth Sci. **9**, 18–35 (1972).
50. J. S. Stacey and I. D. Kramers, "Approximation of Terrestrial Lead Isotope Evolution by a Two-Stage Model," Earth Planet. Sci. Lett. **26**, 207–221 (1975).
51. R. H. Steiger and E. Jager, "Subcomission of Geochronology: Convention of the Use of Decay Constants in Geo- and Cosmochronology," Earth Planet. Sci. Lett. **36**, 359–362 (1976).
52. S.-S. Sun and W. F. McDonough, "Chemical and Isotopic Systematics of Oceanic Basalts," in *Magmatism in Oceanic Basin*, Geol. Soc. Spec. Publ. **42**, 313–345 (1989).
53. S. R. Taylor and S. M. McLennan, *The Continental Crust: Its Composition and Evolution* (Blackwell Publication, Oxford, 1985).
54. E. V. Tolmacheva and S. D. Velikoslavinsky, *Inclusion Studies during Regional Geological Researches and Geological Mapping with Exploration for Minerals in Precambrian Zones: Procedural Instructions* (Vseross. Geol. Inst., St. Petersburg, 1999) [in Russian].
55. L. V. Travin, Extended Abstract of Candidate's Dissertation in Geology and Mineralogy (Vsess. Geol. Inst., Leningrad, 1974).
56. S. D. Velikoslavinsky and V. A. Glebovitsky, "A New Discriminant Diagram for Classification of Island-Arc and Continental Basalts on the Basis of Petrochemical Data," Dokl. Akad. Nauk **401** (2), 1–4 (2005) [Dokl. Earth Sci. **401** (2), 308–310 (2005)].
57. S. D. Velikoslavinsky and V. A. Rudnik, "Geochemistry of Precambrian Volcanism in the Aldan Shield," in *The Geochemistry of BAM Region* (Vsess. Geol. Inst., Leningrad, 1983), pp. 62–83 [in Russian].
58. S. D. Velikoslavinsky, "Geochemical Classification of Silicic Igneous Rocks of Major Geodynamic Environments," Petrologiya **11** (4), 363–380 (2003) [Petrology **11** (4), 327–342 (2003)].
59. S. D. Velikoslavinsky, "Identification of Geodynamic Environments by Petrochemical Characteristics of Basalts," Zap. Vseross. Mineral. O–va **CXXVI** (1), 109–124 (1997).
60. S. D. Velikoslavinsky, Extended Abstract of Doctoral Dissertation in Geology and Mineralogy (St. Petersburg Gos. Univ., St. Petersburg, 1998).
61. S. D. Velikoslavinsky, Extended Abstract of Candidate's Dissertation in Geology and Mineralogy (Vsess. Geol. Inst., Leningrad, 1978).

62. S. D. Velikoslavinsky, V. A. Rudnik, and E. V. Tolmacheva, "Granite Formation, Magmatism, and Metasomatism during the Plate-Tectonic Evolution of the Aldan Shield," in *Metamorphism, Granite Formation, and Ore Genesis* (SPBU, St. Petersburg, 2003), pp. 48–50 [in Russian].
63. S. D. Velikoslavinsky, V. A. Rudnik, and E. V. Tolmacheva, "Metabasalts of the Aldan–Stanovik Shield and the Problem of Early Precambrian Tectonic Regimes," Region. Geol. Metallogeny, No. 4, 38–51 (1995).
64. S. D. Velikoslavinsky, V. A. Rudnik, and E. V. Tolmacheva, "The Volcanic Protoliths of the Enderbite–Crystalline Schist Associations of the Aldan–Stanovik Shield and the Evolution of Basic Volcanism," in *Petrochemical Evolution of Magmatic Associations* (Nauka, Moscow, 1990), pp. 50–67 [in Russian].
65. S. D. Velikoslavinsky, E. V. Tolmacheva, V. L. Dook, *et al.*, "Geochemical Mapping of Basic Complexes in the Early Precambrian Aldan–Stanovoy Shield of Siberia," Precambrian Res. **62** (4), 507–527 (1993).
66. N. I. Verevkin, V. I. Egin, E. M. Zablotskii, and A. R. Entin, "The Archean Stratigraphy of the Central Aldan Shield," in *The Precambrian Geology and Petrology of Aldan Shield* (Nauka, Moscow, 1966), pp. 5–14 [in Russian].